

Optimization of CdSe quantum dot concentration in P3HT:PCBM layer for the improved performance of hybrid solar cells



Eung-Kyu Park^a, Jae-Hyoung Kim^a, In Ae Ji^b, Hye Mi Choi^b, Ji-Hwan Kim^a, Ki-Tae Lim^a, Jin Ho Bang^b, Yong-Sang Kim^{a,*}

^aSchool of Electronic and Electrical Engineering, Sungkyunkwan University, Suwon, Gyeonggi 440-746, Republic of Korea

^bDepartment of Chemistry and Applied Chemistry, Hanyang University, Ansan, Gyeonggi 426-791, Republic of Korea

ARTICLE INFO

Article history:

Received 18 October 2013

Received in revised form 11 April 2014

Accepted 4 May 2014

Available online 14 May 2014

Keywords:

Hybrid solar cell

P3HT:PCBM

CdSe quantum dot

Recombination mechanism

ABSTRACT

The improved performance of hybrid solar cells was obtained due to the effects of CdSe quantum dots (QDs) blended in the active layer. Different concentrations of CdSe QDs were mixed in the poly(3-hexylthiophene):[6,6]-phenyl C₆₁ butyric acid methyl ester (P3HT:PCBM) based active layer. We investigated the effects of CdSe QDs on the solar cell performances by ranging its concentration from 2 to 24 mg/mL. The charge transport in the active layer was improved at the optimized CdSe QDs concentration of 6 mg/mL. The solar cell with pristine active layers showed a 2.98% power conversion efficiency while that with 6 mg/mL CdSe QDs blended in layer showed a higher power conversion efficiency of 3.35% under AM 1.5G illumination. Analysis of recombination mechanism using the current density–voltage (*J*–*V*) characteristic at various light intensities was also performed.

© 2014 Elsevier B.V. All rights reserved.

1. Introduction

The bulk heterojunction (BHJ) solar cells have been a very attractive research area for their advantages like light-weight, flexibility, low-cost, and simple fabrication for large processing area. Amongst the various conductive polymers; high electron mobility and high light absorption coefficient in visible region make polythiophenes a promising candidate as electron donor materials for organic solar cells (OSCs) [1,2]. For increased performance, many researchers have tried to optimize the processing conditions such as solvent, annealing temperature and time, and composition mixture ratio in solvent [3,4]. Recent studies have reported remarkably improved performances of the BHJ solar cells up to 5% of power conversion efficiency (PCE) with poly(3-hexylthiophene):[6,6]-phenyl C₆₁ butyric acid methyl ester (P3HT:PCBM) [5]. However, in the polymer and fullerene blend, the PCE of the devices are limited as the charge carrier mobility is comparatively low, with a short exciton diffusion length in the active layer [6]. In order to improve the performance of OSCs, it is required to introduce other additive nanoparticles.

Nanoparticles help in two ways, metal nanoparticles scatters the light due to surface plasmon resonance (SPR) effects, while inorganic nanoparticles absorbs the light; thereby increasing the

photocurrents of OSCs. It has been extensively studied that the absorbance of nanomaterial can be tuned by changing its size, shape, material, and the ligand [7,8]. Electron transport in nanoparticles is indeed faster than the electron mobility in polymers, which usually have higher hole transport properties [9].

A promising approach to improve light absorption without increasing photoactive layer's thickness is to trap light in the active layer by using inorganic semiconductor based quantum dots such as CdSe QDs. The specific advantage of QDs for light harvesting over organic materials is the quantum confinement effect. It has been extensively reported that the increasing concentration of QDs improves the light absorption property [10]. Depending on the particle size, the energy band gap of CdSe QDs differs. Despite a relatively slow electron injection rate in larger CdSe QDs, the photoelectrode constructed with large nanoparticles exhibits higher energy conversion efficiency than the smaller nanoparticles [11,12]. CdSe QDs based organic/inorganic hybrid solar cells has gained a lot of attention, but this area still needs to be explored deeply [13,14].

The recombination mechanisms in polymer BHJ solar cells are not well established. For P3HT:PC₆₀BM cells, contradictory explanations based on both monomolecular [15,16] and bimolecular [17,18] recombination have been proposed, but have met with only limited success in explaining the current–voltage characteristics. Shockley–Read–Hall (SRH) recombination at interfacial traps [16] was proposed as the dominant mechanism. Monomolecular

* Corresponding author. Tel.: +82 31 299 4323.

E-mail address: yongsang@skku.edu (Y.-S. Kim).

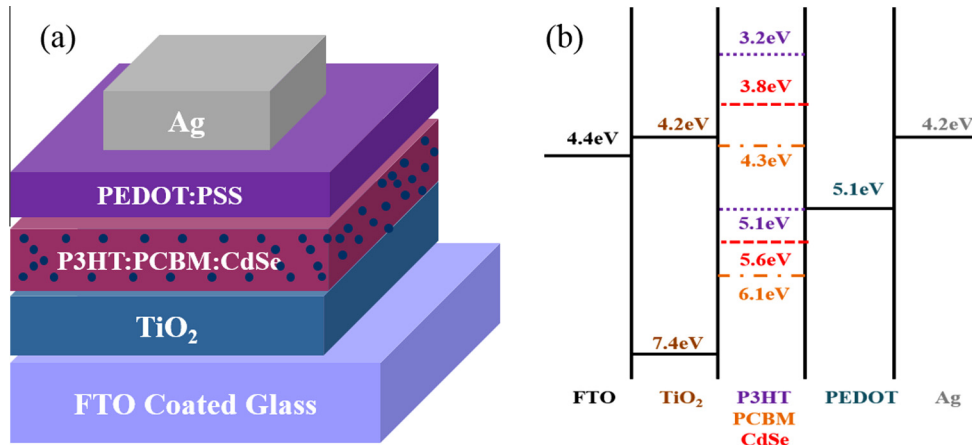


Fig. 1. (a) The schematic of inverted hybrid solar cell. (b) Energy band diagram of the hybrid solar cells with sequential layers of FTO/TiO₂/P3HT:PCBM:(CdSe)/PEDOT:PSS/Ag.

and bimolecular recombination are terms which require precise definition. The intensity dependent current–voltage studies described here determine process order alone. SRH recombination is a monomolecular recombination process in which one electron and one hole recombine through a trap state or recombination center. Impurities in the fullerene and polymer materials and incomplete phase separation interfacial defects that function as traps are likely to contribute to a trap-based recombination.

In this regard, we fabricated P3HT:PCBM:CdSe QDs based ternary hybrid solar cells and optimized the concentration of CdSe QDs in P3HT:PCBM active layer for the highest improvement of solar cell performance. We also validated the role of CdSe QDs in improving the electrical properties by analyzing the external quantum efficiency (EQE), charge collection probability and reduction in the recombination loss.

2. Experimental

We fabricated the solar cell devices with the following structure as shown in Fig. 1(a): FTO/TiO₂/P3HT:PCBM:CdSe/PEDOT:PSS/Ag. In the past we reported that the inverted structure using fluorine-doped tin oxide (FTO) can improve the device performance with higher stability and efficiency [19]. CdSe QDs were prepared by the hot injection method with some modifications. CdO (0.39 mmol), trioctylphosphine oxide (5.2 mmol), and tetradecylphosphonic acid (1.1 mmol) were degassed at 110 °C for 1 h and then heated under nitrogen to 315 °C to completely dissolve the precursors. TOPSe (0.25 mmol Se dissolved in 4.25 mL of trioctylphosphine) was subsequently injected into the hot solution to initiate the reaction. After 5 min of growth at 270 °C, the solution was cooled to room temperature, washed three times with a mixture of methanol and chlorobenzene, for use. The diameter of resulting CdSe particles was 4.5 nm [20].

For the fabrication, FTO glass substrates were cleaned in an ultrasonic bath with acetone, isopropyl alcohol and deionized water for 20 min, respectively. TiO₂ was used as a buffer layer for hole-blocking between the active layer and bottom electrode. TiO₂ solution was spin coated onto FTO substrate and then sintered at 500 °C for 1 h in ambient air condition. The crystallization of P3HT tends to be disturbed when increasing amounts of PCBM is blended in active layer [21,22]. The CdSe QDs (dissolved in 2 mL chlorobenzene) were blended in P3HT:PCBM (40 mg/mL) (P3HT:PCBM = 1:1 weight ratio) in a concentration range of 2–24 mg/mL. The active layer (P3HT:PCBM and P3HT:PCBM:CdSe) was deposited on TiO₂ layer by spin coating.

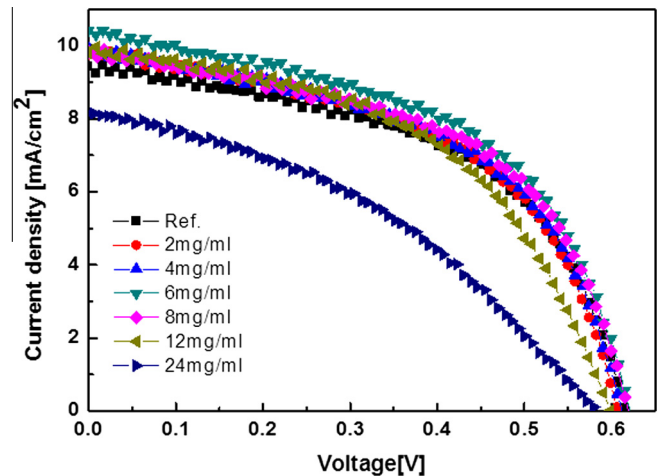


Fig. 2. J - V characteristics of inverted hybrid solar cells using active layer with different concentrations of CdSe QDs under AM 1.5G irradiation at 100 mW/cm².

Table 1

Device performance of hybrid solar cells with different concentration of CdSe QDs, $n = 3$.

CdSe QDs	J_{sc} (mA/cm ²)	V_{oc} (V)	F.F	PCE (%)
Ref.	9.42 (±0.07)	0.61	0.52	2.98
2 mg/mL	9.76 (±0.08)	0.60	0.52	3.04
4 mg/mL	9.91 (±0.09)	0.61	0.51	3.08
6 mg/mL	10.42 (±0.05)	0.62	0.52	3.35
8 mg/mL	9.82 (±0.09)	0.61	0.52	3.23
12 mg/mL	9.82 (±0.08)	0.59	0.49	2.92
24 mg/mL	8.12 (±0.18)	0.58	0.38	1.83

The thickness of the active layer in this case was 75 nm (measured by alpha-step). In order to deposit hydrophilic PEDOT:PSS solution onto a hydrophobic active layer, PEDOT:PSS was mixed with 0.5 vol% of Triton X-100 (C₁₄H₂₂O(C₂H₄O)_n) nonionic surfactant. Then this solution was spin coated on hexamethyldisilazane pre-coated surface of the active layer. Thermal pre-annealing was conducted in 160 °C for 10 min in a dry oven with ambient nitrogen. Finally, Ag top electrode (100 nm) was deposited on PEDOT:PSS layer by thermal evaporation, defining an active area of 0.1 cm². The current density–voltage (J - V) characteristic was measured by a J - V curve tracer (Eko MP-160) and solar simulator (Yss-E40, Yamashita Denso) under AM 1.5G (100 mW/cm²)

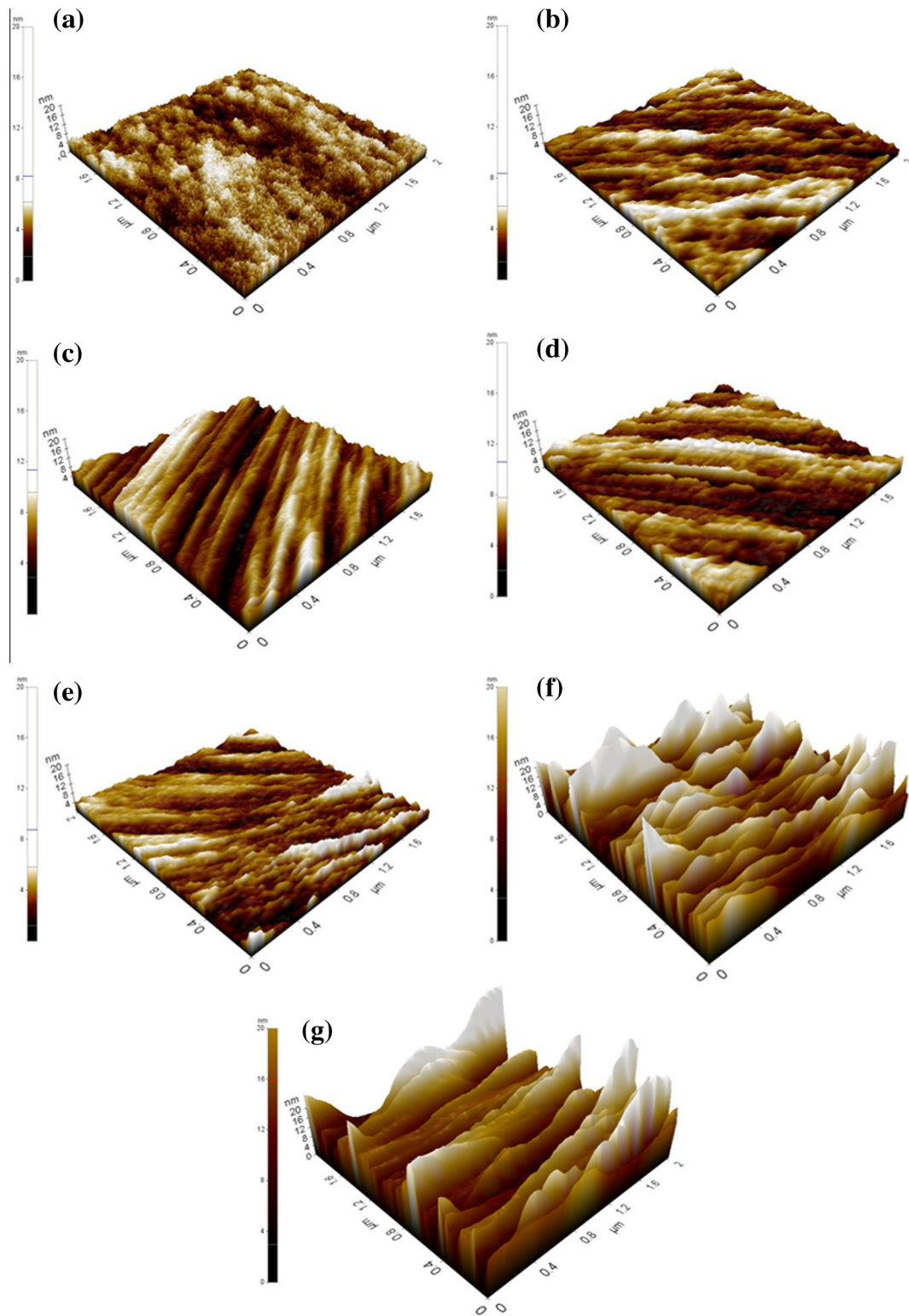


Fig. 3. AFM images of P3HT:PCBM:(CdSe) layer with different concentrations of CdSe QDs (a) P3HT:PCBM, (b) 2 mg/mL, (c) 4 mg/mL, (d) 6 mg/mL, (e) 8 mg/mL, (f) 12 mg/mL, (g) 24 mg/mL.

irradiation intensity. External quantum efficiency (EQE) spectra was measured under calibrated, monochromatic light illumination obtained from a xenon light source operating in the wavelength range of 400–700 nm (K3100, Mc Science). The light intensity was calibrated with a standard silicon cell (PV Measurements, Inc.). The output voltage of solar cells depends on the intensity of

light. To study this dependency, we altered the illumination intensity of solar simulator, by varying the power of the lamp power supply. The intensity of the illumination was checked every time before the measurement with a calibrated silicon cell and meter. Entire fabrication and measurement processes were conducted in ambient air.

3. Results and discussions

The measured $J-V$ characteristics of hybrid solar cells using P3HT:PCBM and P3HT:PCBM:CdSe (different concentration) are shown in Fig. 2. The bare device showed a short circuit current density (J_{sc}) of 9.42 mA/cm². The addition of 2 mg/mL CdSe QDs elevated the J_{sc} to 9.76 mA/cm². Increasing concentration of CdSe QDs resulted in higher current density. It can be observed that the highest performance was shown by the device with 6 mg/mL of CdSe QDs. In this case the device gave a J_{sc} of 10.42 mA/cm² while the device with 24 mg/mL showed a lower J_{sc} of 8.12 mA/cm². The exciton generation was proportionate to light absorption in the active layer. Fig. 1(b) shows the energy band diagram of ternary component-based solar cells. The HOMO and LUMO of QDs exists between those of acceptor material (P3HT) and donor material (PCBM). It is expected that, upon the incidence of light, both P3HT and CdSe absorb photons and generate excitons. This results in electron transfer from the polymer to CdSe or PCBM and from CdSe to PCBM; and hole injections from CdSe to the

polymer. The hole transport is accomplished by the polymer, while the electrons are transported in the PCBM phase. The ability of TOPO-capped CdSe nanoparticles to absorb light and inject electrons in C60 has been shown by Biebiersdorf et al. [23,24] and corroborates the mechanism proposed here.

The average performances of solar cells ($n = 3$) with different concentrations of CdSe QDs are summarized in Table 1. Repeated trials of the work showed a low average standard deviation of 0.095 for the J_{sc} data. Use of 6 mg/mL QDs helped in the faster electron transfer [25,26], resulting in increased short circuit current density by 10%. However, much higher concentration of CdSe QDs reduced the open circuit voltage (V_{oc}) as it is assumed that the energy band of CdSe QDs directly bonds with that of P3HT:PCBM. The CdSe QDs concentration of 12 and 24 mg/mL also reduced the fill factor (F.F) and open circuit voltage (V_{oc}) because of a highly rough surface. As shown in Fig. 3, the P3HT:PCBM active layer without CdSe QDs has an RMS surface roughness of 2.78 nm and CdSe QDs blended layer with concentration of 2, 4, 6, 8, 12, and 24 mg/mL has an increased RMS surface roughness of 2.87, 3.21, 3.78, 4.95, 11.5, and 13.36 nm, respectively. The coarse morphology of the blended film consequence in poor contact between the active layer and cathode and increases the resistance. Bumpy surface also reflects light away from the device.

In our previous work, we reported that the rough surface reduces the efficiency of OSCs [27]. A very high concentration of CdSe QDs destabilized the surface energy of layer leading to a protruded structure. This change in surface morphology eventuated in a deteriorated device efficiency. The active layer with a CdSe concentration of 6 mg/mL showed the optimal current density.

Fig. 4 shows the measured external quantum efficiency (EQE) of OSCs. A comparison of the increase in EQE between pristine and the CdSe QDs blended device was done. The device showed enhanced quantum efficiency in the broad wavelength range due to adequate absorption of light. The photocurrent within the wavelength range from 400 to 700 nm increased significantly after addition of the CdSe QDs. A 38% increase in EQE was obtained due to 6 mg/mL CdSe QDs in the active layer. The improvement of J_{sc} as shown in Fig. 2 can be verified by the EQE results. Fig. 5(a) shows the semi log plot of dependence of open circuit voltage on the light intensity. At open circuit voltage, V_{oc} , the photocurrent is zero and all photo generated carriers recombine within the cell. Thus,

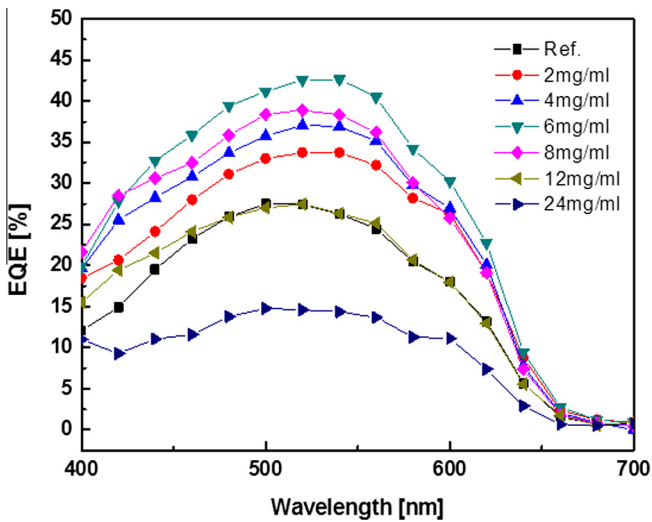


Fig. 4. External quantum efficiency characteristics of inverted hybrid solar cells using active layer with different concentrations of CdSe QDs.

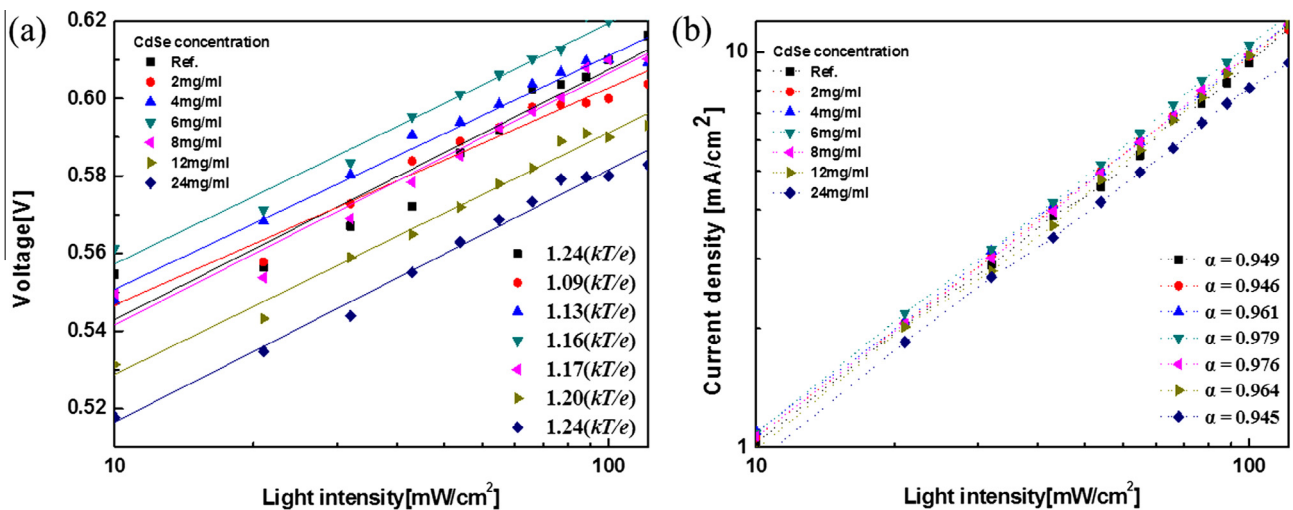


Fig. 5. (a) The measured V_{oc} of hybrid solar cells with different concentration of CdSe as a function of illumination intensity (symbols), together with linear fits of the data (solid lines). (b) Measured J_{sc} of hybrid solar cells with different concentration of CdSe plotted against light intensity (symbols) on the logarithmic scale and fitted yield α (dotted line).

recombination studies at V_{OC} can provide detailed information of various mechanisms. The relationship between light intensity and V_{OC} is given by [28,29]:

$$\delta V_{OC} = \frac{kT}{e} \ln(I) + const. \quad (1)$$

where k is the Boltzmann constant, T is the temperature, e is the electronic charge and I is the incident light intensity. When the additional mechanism of SRH trap-assisted recombination is involved, a stronger dependence of V_{OC} on light intensity with a slope greater than kT/e is observed [28]. The higher value of the slope coefficient is associated with the strength of trap-assisted recombination. The bare device showing a slope of $1.24(kT/e)$ is indicative of trap-assisted recombination. The addition of 2 mg/mL CdSe QDs decreased the slope value to $1.09(kT/e)$. At a concentration of 24 mg/mL, the increased value of slope to $1.24(kT/e)$ indicates an increase in the strength of the trap-assisted recombination. Implying that the CdSe QDs reduced the density of traps between the active layer and Ag contact, and hence SRH recombination is suppressed. However, low concentration of CdSe QDs carefully passivates the P3HT:PCBM tailing and stops trap-assisted recombination.

The J_{sc} can be correlated to light intensity (I) by [30],

$$J_{sc} \propto I^\alpha (\alpha \leq 1) \quad (2)$$

At short circuit, the bimolecular recombination should be minimum ($\alpha \approx 1$) for maximum carrier sweep out. Any deviation from $\alpha \approx 1$ implies bimolecular recombination. Fig. 5(b) shows the log–log scale relationships of J_{sc} as a function of light intensity, calculated using the power law described above. The fitting of the data yielded $\alpha = 0.949$ for bare device, which can be attributed to the bimolecular recombination. It can be observed that the highest performing hybrid solar cells with 6 mg/mL CdSe QDs gave an α value of 0.979, while the device with 24 mg/mL showed a decreased α value of 0.945. The J_{sc} vs. I data prove the J – V characteristics as shown in Fig. 2, because the bimolecular recombination is close to minimum at short circuit current density [30].

4. Conclusion

The effect of CdSe QDs in P3HT:PCBM:CdSe ternary system OSCs was investigated. We studied the effect of CdSe QDs by ranging its concentration from 2 to 24 mg/mL. Different concentration of CdSe QDs showed different short circuit current density due to the charge transport property. The CdSe QDs concentration of 6 mg/mL in the active layer resulted in enhanced performance. The solar cells with a pristine active layer showed a 2.98% efficiency, mono-molecular slope $1.24(kT/e)$ and bimolecular 0.949 while 6 mg/mL CdSe QDs blended layer showed a higher performance of 3.35%, slope $1.16(kT/e)$, 0.979 recombination property under AM 1.5G illumination. On the other hand, a very high concentration of CdSe QDs disturbed the electrical property of the device.

Acknowledgment

This work was supported by the Human Resources Development program (No. 20124010203280) of the Korea Institute of Energy Technology Evaluation and Planning (KETEP) Grant funded by the Korea Government Ministry of Trade, Industry and Energy.

References

- [1] Y. Zhou, M. Eck, C. Veit, B. Zimmermann, F. Rauscher, P. Niyamakom, S. Yilmaz, I. Dumsch, S. Allard, U. Scherf, M. Kruger, *Sol. Energy Mater. Sol. Cells* 95 (2011) 1232–1237.
- [2] M. Helgesen, R. Sondergaard, F.C. Krebs, *J. Mater. Chem.* 20 (2010) 36–60.
- [3] W.H. Baek, H. Yang, T.S. Yoon, C.J. Kang, H.H. Lee, Y.S. Kim, *Sol. Energy Mater. Sol. Cells* 90 (2009) 1263–1267.
- [4] G. Li, Y. Yao, H. Yang, V. Shirotriya, G. Yang, Y. Yang, *Adv. Funct. Mater.* 17 (2007) 1636–1644.
- [5] K. Kim, J. Liu, M.A.G. Namboothiry, D.L. Carroll, *Appl. Phys. Lett.* 90 (2007) 163511.
- [6] K.M. Coakley, M.D. McGehee, *Chem. Mater.* 16 (2004) 4533–4542.
- [7] J.J. Mock, M. Barbic, D.R. Smith, D.A. Schultz, S. Schultz, *J. Chem. Phys.* 116 (2002) 6755–6759.
- [8] G. Xu, M. Tazawa, P. Jin, S. Nakao, K. Yoshimura, *Appl. Phys. Lett.* 82 (2003) 3811–3813.
- [9] V. Coropceanu, J. Cornil, D.A. da Silva Filho, Y. Olivier, R. Silbey, J.L. Brédas, *Chem. Rev.* 107 (2007) 926.
- [10] H. Lee, M. Wang, P. Chen, D.R. Gamelin, S.M. Zakeeruddin, M. Gratzel, M.K. Nazeeruddin, *Nano Lett.* 9 (2009) 4221–4227.
- [11] E.M. Boatman, G.C. Lisensky, K.J. Nordell, *J. Chem. Educ.* 82 (2005) 1697–1699.
- [12] J. Bang, P.V. Kamat, *ACS Nano* 5 (2011) 9421.
- [13] W.U. Huynh, J.J. Dittmer, A.P. Alivisatos, *Science* 295 (2002) 2425–2427.
- [14] N.T.N. Truong, W.K. Kim, C. Park, *Sol. Energy Mater. Sol. Cells* 95 (2011) 167–170.
- [15] D. Veldman, O. Ipek, S.C.J. Meskers, J. Sweelssen, M.M. Koetse, S.C. Veenstra, J.M. Kroon, S.S. van Bavel, J. Loos, R.A.J. Janssen, *J. Am. Chem. Soc.* 130 (2008) 7721–7735.
- [16] R.A. Street, M. Schoendorf, A. Roy, J.H. Lee, *Phys. Rev. B* 81 (2010) 205307.
- [17] C. Groves, N.C. Greenham, *Phys. Rev. B* 78 (2008) 155205.
- [18] C.G. Shuttle, B. O'Regan, A.M. Ballantyne, J. Nelson, D.D.C. Bradley, J.R. Durrant, *Phys. Rev. B* 78 (2008) 113201.
- [19] W.H. Baek, M. Choi, T.S. Yoon, H.H. Lee, Y.S. Kim, *Appl. Phys. Lett.* 96 (2010) 133506.
- [20] W.W. Yu, L. Qu, W. Guo, X. Peng, *Chem. Mater.* 15 (2003) 2854–2860.
- [21] P. Vanlaeke, A. Swinnen, I. Haeldermans, G. Vanhoyland, T. Aernouts, D. Cheyns, C. Deibel, J. D'Heaen, P. Heremans, J. Poortmans, J.V. Manca, *Sol. Energy Mater. Sol. Cells* 90 (2006) 2150–2158.
- [22] W.H. Baek, T.S. Yoon, H.H. Lee, Y.S. Kim, *Org. Electron.* 11 (2010) 933–937.
- [23] A. Biebiersdorf, R. Dietmüller, A.S. Susha, A.L. Rogach, S.K. Poznyak, D.V. Talapin, H. Weller, T.A. Klar, J. Feldmann, *Nano Lett.* 6 (2006) 1559.
- [24] J.N.D. Freitas, I.R. Grova, L.C. Akcelrud, E. Arici, N.S. Sariciftci, A.F. Nogueira, *J. Mater. Chem.* 20 (2010) 4845–4853.
- [25] H. Derbal-Habak, C. Bergeret, J. Cousseau, J.M. Nunzi, *Sol. Energy Mater. Sol. Cells* 95 (2011) 553–556.
- [26] L. Irina, R. Nikolay, K.O. Joanna, *J. Phys. Chem. C* 114 (2010) 12784–12791.
- [27] G. Li, V. Shirotriya, J. Huang, Y. Yao, T. Moriarty, K. Emery, Y. Yang, *Nat. Mater.* 4 (2005) 864–868.
- [28] S.R. Cowan, A. Roy, A.J. Heeger, *Phys. Rev. B* 82 (2010) 245207.
- [29] L.J.A. Koster, V.D. Mihailetschi, R. Ramaker, P.W.M. Blom, *Appl. Phys. Lett.* 86 (2005) 123509.
- [30] I. Riedel, J. Parisi, V. Dyakonov, L. Lutsen, D. Vanderzande, J.C. Hummelen, *Adv. Funct. Mater.* 14 (2004) 38–44.